Identification of a Novel Chloroplast Protein AtNYE1 Regulating Chlorophyll Degradation during Leaf Senescence in Arabidopsis[1][C][W][OA]

Guodong Ren, Kun An, Yang Liao, Xiao Zhou, Yajun Cao, Huifang Zhao, Xiaochun Ge, and Benke Kuai*

State Key Laboratory of Genetic Engineering, Department of Biochemistry, School of Life Sciences, Fudan University, Shanghai 200433, China

A dramatic increase of chlorophyll (Chl) degradation occurs during senescence of vegetative plant organs and fruit ripening. Although the biochemical pathway of Chl degradation has long been proposed, little is known about its regulatory mechanism. Identification of Chl degradation-disturbed mutants and subsequently isolation of responsible genes would greatly facilitate the elucidation of the regulation of Chl degradation. Here, we describe a nonyellowing mutant of Arabidopsis (*Arabidopsis thaliana*), *nye1-1*, in which 50% Chl was retained, compared to less than 10% in the wild type (Columbia-0), at the end of a 6-d dark incubation. Nevertheless, neither photosynthesis- nor senescence-associated process was significantly affected in *nye1-1*. Characteristically, a significant reduction in pheophorbide *a* oxygenase activity was detected in *nye1-1*. However, no detectable accumulation of either chlorophyllide *a* or pheophorbide *a* was observed. Reciprocal crossings revealed that the mutant phenotype was caused by a monogenic semidominant nuclear mutation. We have identified *AtNYE1* by positional cloning. Dozens of its putative orthologs, predominantly appearing in higher plant species, were identified, some of which have been associated with Chl degradation in a few crop species. Quantitative polymerase chain reaction analysis showed that *AtNYE1* was drastically induced by senescence signals. Constitutive overexpression of *AtNYE1* could result in either pale-yellow true leaves or even albino seedlings. These results collectively indicate that NYE1 plays an important regulatory role in Chl degradation during senescence by modulating pheophorbide *a* oxygenase activity.

Ever since the nonyellowing mutant was identified, chlorophyll (Chl) catabolism has been known as a separable event from other senescence processes in senescing vegetative plant organs and ripening fruits (Thomas and Stoddart, 1975; Thomas and Howarth, 2000). Extensive chemical and biochemical analyses have led to the construction of a major Chl catabolism pathway, i.e. pheophorbide *a* oxygenase (PaO) pathway (Hörtensteiner, 2006; Tanaka and Tanaka, 2006). However, very little is known about its regulation. According to the proposed pathway, phytol and magnesium (Mg) are first removed from Chl *a* by chlorophyllase (Chlase) and a putative Mg-dechelatase or Mg-dechelating substance, respectively, and the resultant pheophorbide *a* (Pheide *a*) is then converted to the primary fluorescent Chl catabolites (pFCCs) through the sequential functioning of two enzymes: PaO and red Chl catabolite reductase (RCCR). The pFCC is subsequently transported out of the chloroplast and converted to the colorless nonfluorescent Chl catabolites in the vacuole. Chl *b* is proposed to be transformed to Chl *a* with a two-step reduction, catalyzed by Chl *b* and 7[1]-OH-Chl *a* reductases, respectively, before being further degraded (Tanaka and Tanaka, 2006). Over the past few years, the identification of genes encoding key enzymes, including *CLH*s (for chlorophyll-chlorophyllido hydrolases), *PaO*, and *RCCR*, offered a possibility of exploring the regulation of Chl catabolism (Gray et al., 1997; Jacob-Wilk et al., 1999; Tsuchiya et al., 1999; Wüthrich et al., 2000; Pružinská et al., 2003). Of the three genes identified, *PaO* is thus far shown to have a regulatory effect on Chl degradation (Pružinská et al., 2003; Pružinská et al., 2005; Chung et al., 2006). Nevertheless, a mutation in *PaO* or even a down-regulation of *PaO* expression may cause a lesion mimic phenotype, a reaction resembling the hypersensitive response induced by pathogens.

An alternative way to explore the regulatory mechanism of Chl catabolism is to identify genes directly regulating Chl degradation during senescence through forward genetics. Mutants, with Chl degradation being disturbed but other senescence-associated processes not being significantly affected, have been reported in diversified species (Thomas and Stoddart, 1975; Guiamét et al., 1990; Akhtar et al., 1999; Cha et al.,

[1] This work was supported by the National Science Foundation of China (grant no. 39870452).

* Corresponding author; e-mail bkkuai@fudan.edu.cn; fax 86–21–65642648.

The author responsible for distribution of materials integral to the findings presented in this article in accordance with the policy described in the Instructions for Authors (www.plantphysiol.org) is: Benke Kuai (bkkuai@fudan.edu.cn).

[C] Some figures in this article are displayed in color online but in black and white in the print edition.

[W] The online version of this article contains Web-only data.

[OA] Open Access articles can be viewed online without a subscription.

www.plantphysiol.org/cgi/doi/10.1104/pp.107.100172

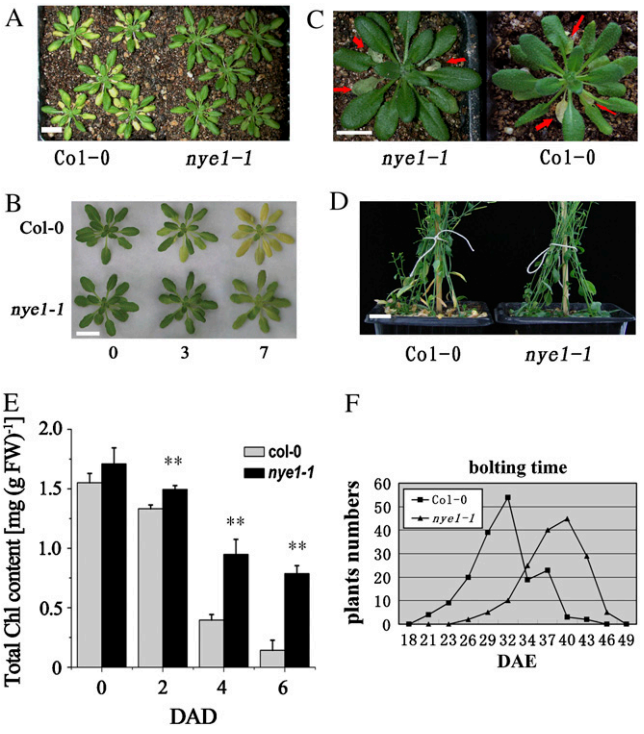

Figure 1. Phenotypic characterization of *nye1-1*. A, Three-week-old plants were incubated in permanent darkness for 4 d. B, Differential changing patterns in yellowing phenotypes between *nye1-1* and Col-0 plants, as well as between young and old leaves, with roots removed, during a 7-d incubation in darkness, as described in "Materials and Methods." C and D, Nonyellowing senescent leaves (red arrows) of *nye1-1*, compared to the yellowing ones of Col-0, 30 (C) and 45 (D) d after germination, respectively. Bar = 1 cm. E, Changes in the levels of total Chl in *nye1-1* and Col-0 leaves during a 6-d dark incubation. Data are means of three replicates. Error bars indicate SD. The experiment was repeated twice with almost the same results. DAD represents day(s) after darkness. Statistical analysis of differences in *nye1-1* with respect to Col-0 was performed using two-tailed *t* test. The significant difference is denoted with two asterisks ($P < 0.01$). F, *nye1-1* bolts some a week later than Col-0 under long-day conditions.

2002; Guiamét et al., 2002; Luquez and Guiamét, 2002; Oh et al., 2003, 2004; Efrati et al., 2005). But only quite recently have the identities of corresponding genes been indicated in two crop species, *Festuca pratensis* and rice (*Oryza sativa*; Armstead et al., 2006; Hörtensteiner, 2006). However, there has been so far no genetic confirmation of cloning of the responsible genes.

Here we report the isolation of a nonyellowing mutant (*nye1-1*) from a fast-neutron mutagenized M2 population of Arabidopsis (*Arabidopsis thaliana*). It was shown that the mutation primarily affected Chl catabolism, mainly by reducing PaO activity, during senescence. However, no detectable accumulation of major Chl degradation intermediates was observed in *nye1-1*. We isolated the causal gene *AtNYE1* by positional cloning and confirmed its identity by genomic complementation. Overexpression of *AtNYE1* may cause either pale-yellow true leaves or even albino seedlings.

RESULTS

Isolation and Phenotypic Characterization of *nye1-1*

To explore the regulatory mechanism of Chl degradation during leaf senescence, a nonyellowing mutant was identified from the M2 population of fast-neutron mutagenized Arabidopsis (Columbia-0 [Col-0]). It was subsequently backcrossed with Col-0 four times and designated as *nye1-1* (nonyellowing). The *nye1-1* mutant exhibited a stable nonyellowing phenotype during both natural and dark-induced senescence of leaves either attached, detached, or in planta (Figs. 1, A–D, and 2A). Its siliques also stayed lightly green at harvesting time (Supplemental Fig. S1). In all the follow-up experiments, incubating detached leaves in darkness was therefore adopted constantly as the simplest way to identify the mutation phenotype. Under long-day (16-h light/8-h dark) growth condition, an approximately 9-d delayed bolting and a slightly prolonged flowering period were observed in *nye1-1*, as compared with Col-0 (Fig. 1F). No other significant morphological differences were observed between *nye1-1* and Col-0, and the etiolation/deetiolation behavior was not altered either (data not shown).

In reciprocal crosses with the wild types of both the Col-0 and Landsberg *erecta* (L*er*), all the leaves of F1 plants showed a partially stay-green phenotype after 4-d dark treatment (Fig. 2A). Total Chl content of F1 plants was significantly higher ($P < 0.01$) than that of

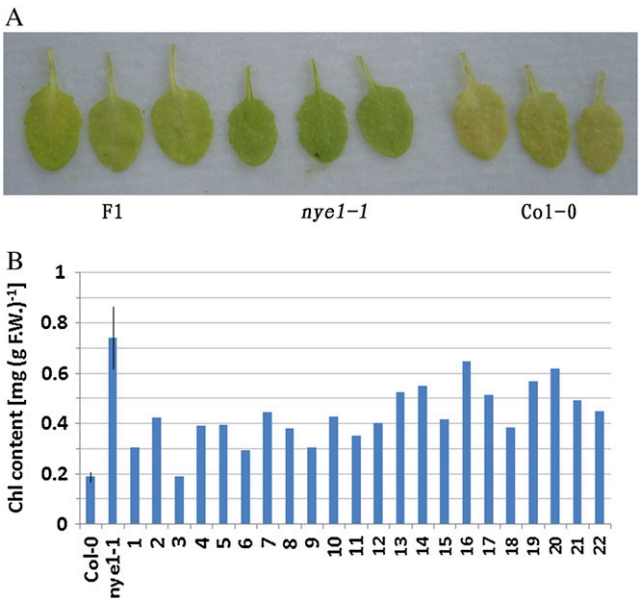

Figure 2. Semidominant phenotype of F1. A, Detached leaves treated in darkness for 4 d. Bar = 1 cm. B, Spectrophotometric analysis of total Chl content of F1 lines. Three leaf discs (4–6 true leaves) were weighed and incubated in darkness before the determination. Numerals 1 to 22 indicate 22 individual F1 lines. For *nye1-1* and Col-0 controls, data represent the means of four replicates. Error bars indicate SD. The experiment was repeated once with similar results. [See online article for color version of this figure.]

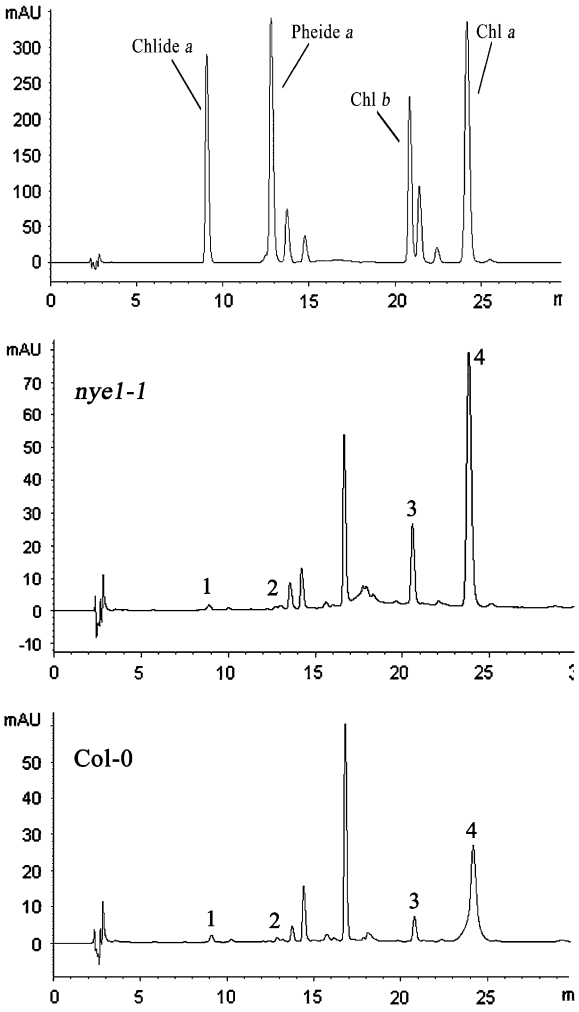

Figure 3. Representative data of relative changes in the contents of green pigments in the leaves of *nye1-1* and Col-0 after a 4-d dark incubation, monitored by HPLC. Numerals 1 to 4 indicate Chlide *a*, Pheide *a*, Chl *b*, and Chl *a*, respectively. Peaks unnumbered possibly represent carotenoid derivatives. The experiment was repeated twice.

wild-type plants after 4-d dark treatment and lower ($P < 0.01$) than that of mutants (Fig. 2B). A statistical 1:2:1 segregation ratio was detected in the F2 population (backcrossed to Col-0; 44 wild-type phenotype:64 mutant phenotype:131 intermediate phenotype; $\chi^2 = 5.56$, $P = 0.062 > 0.05$), and a consistent result was also observed in the F2 population of crosses to L*er* (data not shown). Thus, we concluded that the mutant phenotype was caused by a monogenic semidominant nuclear mutation.

A Reduced PaO Activity But No Detectable Accumulation of Green Catabolites in *nye1-1* during Dark Treatment

To detect the lesion step of Chl degradation, total pigments were extracted from the leaves of *nye1-1* as well as Col-0, and initially quantified by spectrophotometry. Over the course of a 6-d dark treatment, the Chl content declined dramatically in the leaves of Col-0, down to approximately 10% of that in the untreated leaves by the end of the treatment. By contrast, the Chl content in *nye1-1* dropped much more slowly, 50% of that in the untreated leaves being retained at day 6 (Fig. 1E). The result was further validated by HPLC analysis (data not shown). However, no significant accumulation of either chlorophyllide *a* (Chlide *a*) or Pheide *a* was observed either in *nye1-1* or in Col-0 in the chromatogram assay, although trace levels of the above catabolites were detected in both of the genotypes after 0-, 2-, and 4-d dark treatment (Fig. 3 indicates representative data of 4-d samples). To gain insight into the mechanism of the delayed Chl degradation, time-course changes in the transcript levels of *AtCLH1*, *PaO*, and *RCCR* were examined during dark treatment and no differences were detected either between the two genotypes (Fig. 4). Nevertheless, subsequent analyses of in vivo key enzyme activities known for green pigment degradation revealed that the function of PaO in *nye1-1* was somehow reduced, while Chlase remained fully competent (Fig. 5, A and B). pFCC-1 was hardly detected at 0 d after darkness in both *nye1-1* and Col-0 in a coupled PaO-RCCR enzymatic assay. The PaO activity in *nye1-1*, although also dramatically induced, was significantly lower (20% to approximately 50% residual activity relative to that in Col-0 in repeated experiments) than that in Col-0 (Fig. 5B; Table I). A crossover experiment (Roca et al., 2004) was also employed to exclude the possibility that the nonyellowing phenotype in *nye1-1* was due to a lesion in the RCCR activity. Our results clearly demonstrated that the RCCR in *nye1-1* was fully competent (Table I). These data suggest that NYE1 may have a function in modulating the PaO activity, either directly or indirectly, on its cleavage of the porphyrin ring.

Photosynthesis- and Senescence-Associated Processes Largely Unaffected in the Leaves of *nye1-1*

To elucidate the possible relationship of the nonyellowing mutation with photosynthesis, the photosynthetic capacity was initially examined in both genotypes. Compared with that in Col-0, a substantially identical changing pattern of the net photosynthetic rate in the fourth to sixth leaves was observed in *nye1-1* in a time-course monitoring experiment. The photosynthetic rates started to decline slightly 15 d after emergence (DAE), dramatically 21 DAE and sharply 27 DAE in the leaves of both genotypes (Fig. 6A). To explore the relationship further, the transcriptions of two photosynthesis-associated genes, Chl *a*/*b*-binding (*CAB*) protein gene and ribulose bisphosphate carboxylase/oxygenase small subunit (*RBCS*) gene, were examined by quantitative PCR (qPCR). The transcript levels of *CAB* declined sharply during dark-induced senescence, but indistinguishably between *nye1-1* and Col-0 (Fig. 6B). The transcript levels of *RBCS* also declined rapidly in Col-0, but less dramatically in *nye1-1* (Fig. 6C). To determine whether senescence processes are affected by

the mutation, the transcript levels of two well-characterized senescence-associated genes, *SEN1* and *SAG12*, were examined in both *nye1-1* and Col-0. Increased abundances of both *SEN1* and *SAG12* transcripts were detected in both the genotypes after a 2-d dark treatment in a similar way (Fig. 6, D and E). These results indicated that neither photosynthesis- nor senescence-associated processes were significantly affected by the mutation. The *nye1-1* could therefore be classified as a nonfunctional (type C) stay-green mutant (Thomas and Howarth, 2000).

Mapping and Isolation of *AtNYE1*

Twenty-two simple sequence length polymorphic (SSLP) markers (http://www.arabidopsis.org), distributed evenly on five chromosomes, were employed

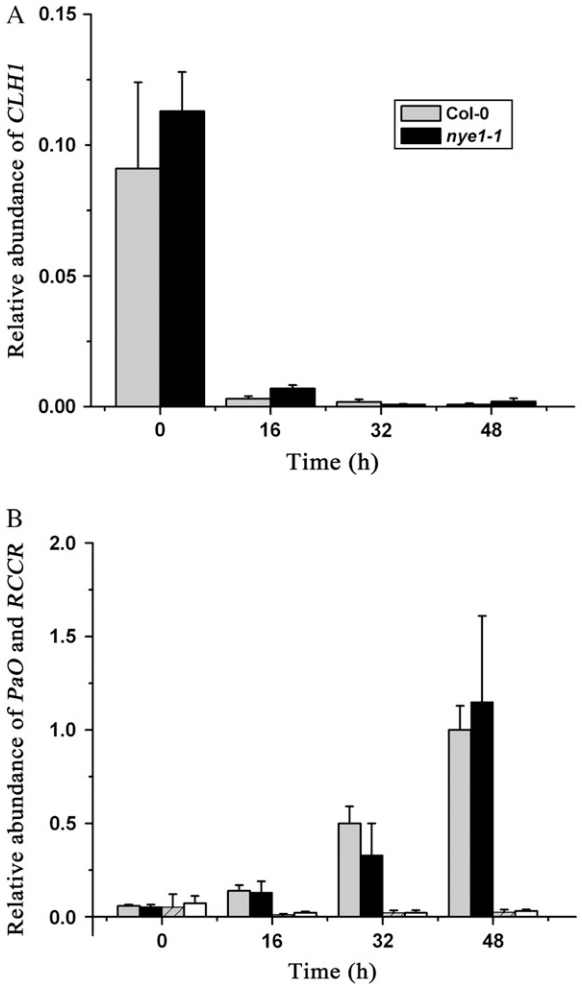

Figure 4. Transcript levels of related enzyme-encoded genes in *nye1-1*. A, Changes in the transcript levels of *AtCLH1* in both *nye1-1* and Col-0 during a dark incubation. B, Changes in the transcript levels of *PAO* and *RCCR* during a dark incubation. Gray, *PaO* (wild type); black, *PaO* (*nye1-1*); hatched gray, *RCCR* (wild type); white, *RCCR* (*nye1-1*). Transcript levels quantified by real-time reverse transcription (RT)-PCR with *ACTIN2* as the reference. Values are means of three replicates. Error bars indicate SD. The experiment was repeated once with similar results.

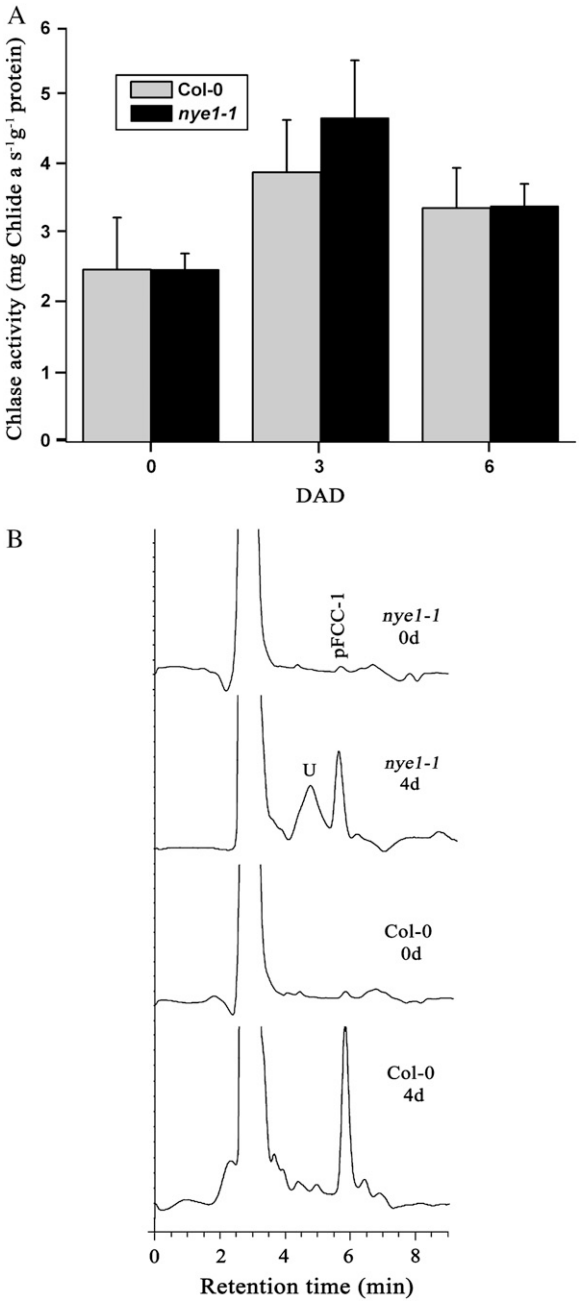

Figure 5. Activities of Chl degradation related enzymes in *nye1-1* and Col-0. A, Changes in Chlase activity during a 6-d dark incubation. Chlase activity in crude enzyme extracts from both *nye1-1* and Col-0 was measured on day 0, 3 and 6 d after incubation in darkness and normalized to their protein contents. Values are means of three replicates. Error bars indicate SD, and DAD represents day(s) after darkness. B, HPLC analysis of PaO-RCCR coupled assay with crude extraction of PaO and RCCR from *nye1-1* and Col-0 leaves during a 4-d dark treatment; pFCC-1 was eluted after 5.8 min, as indicated. U, Unknown peak. The large early peak was due to NADPH present in the reaction mixture. The experiment was repeated once with qualitatively identical results.

Table I. *Crossover analysis of PaO-RCCR activity in nye1-1*

Senescent leaf tissues (detached, 5-d darkness) from both genotypes were used for crude extraction of PaO and RCCR. Reaction mixtures containing all necessary cofactors were incubated at 25°C for 1 h and stopped by cold methanol. FU, Fluorescence unit. Experiment was repeated once and the result was qualitatively identical.

Washed Membrane Proteins (Source of PaO)	S1 Stroma Fraction (Source of RCCR)	pFCC-1 FU h^{-1} g^{-1} Fresh Weight (Peak Area [μV·s])
Col-0	Col-0	9.6E6
Col-0	*nye1-1*	9.0E6
nye1-1	*nye1-1*	2.4E6
nye1-1	Col-0	2.0E6

to map *NYE1* locus, with a mixed DNA sample extracted separately from 100 homozygous individuals identified from an F2 population derived from a cross with wild-type L*er*. The locus was roughly located between F7J7 and F10N7, with an interval of approximately 8.0 cM on the long arm of chromosome IV. New SSLP markers within this region were generated to narrow down the interval. With a mapping population of 828 plants, the locus was further located between T12H17 and F7H19, with an interval of 0.5 cM (Fig. 7).

Sequencing the middle region of approximately 40 kb within this interval led to the identification of a single base pair change, an A to T substitution, at position 29 of the first exon in the open reading frame (ORF) of at4g22920. This mutation converts the 10th Leu to a stop codon, which leads to an early termination of the translation. The at4g22920 was therefore tentatively designated as *AtNYE1*.

Complementation of *nye1-1* Phenotype by the Genomic Copy of *AtNYE1*

A 4.1-kb *Pst*I-*Bam*HI genomic fragment, containing *AtNYE1* as well as its 1.9 kb upstream and 1.0 kb downstream sequences, was amplified and constructed into pPZP221 (Hajdukiewicz et al., 1994), which was subsequently introduced into *Agrobacterium tumefaciens* strain LBA4404. Plants of *nye1-1* were transformed using standard dipping method (Clough and Bent, 1998). In the first batch of selection, 11 gentamycin-resistant plants were selected and their transgenic status was confirmed by PCR (data not shown). The leaves of these transgenic plants showed a rapid yellowing phenotype during natural aging and dark-induced senescence, just as those of Col-0 did (Fig. 8, A and B). The complementation results not only confirmed the genetic function of *AtNYE1*, but also indicated that the 4.1-kb genomic fragment was sufficient to regulate Chl degradation.

Overexpression of *AtNYE1* Caused Precocious Chl Degradation

To examine its capacity in regulating Chl degradation, we expressed *AtNYE1*, driven by cauliflower mosaic virus 35S promoter, in *nye1-1*. Fifty transgenic seedlings were obtained in the first batch. Of them, 21 developed normally, 11 showed pale-yellow true leaves displaying varied degrees of degreening, and the rest (18) exhibited albino phenotype (Fig. 9, A and B). The severity of the degreening in the *AtNYE1* overexpressors was not only reflected on retardation to their growth and development but also well correlated with the expression level of *AtNYE1* (Fig. 9C). In addition, we also detected that *PaO* expression was not induced in these overexpression lines (Fig. 9C), indicating that a higher expression of *AtNYE1* is sufficient to induce Chl degradation, provided that there is a basal level of *PaO* expression.

AtNYE1 Gene Encodes a Novel Protein Highly Conserved in Plants

AtNYE1 encodes a 268-amino acid protein with an apparent molecular mass of 30 kD and a theoretical pI of 8.73 (Fig. 10A). ChloroP analysis (http://www.cbs.dtu.dk/services/ChloroP/; Emanuelsson et al., 1999) suggested that AtNYE1 contains a putative chloroplast transit peptide in the N-terminal region (residues 1–48).

Searching of the GenBank database (http://www.ncbi.nlm.nih.gov/BLAST) and The Institute of Genomic Research plant genome database (http://www.tigr.org/plantProjects.shtml) revealed dozens of ESTs that are highly homologous to *AtNYE1* in diversified species of angiosperms and gymnosperms, but not in yeast (*Saccharomyces cerevisiae*) and animals (Fig. 10A). Putative genes that encode proteins showing weak similarities to AtNYE1 are also present in a green algae, *Ostreococcus tauri* (CAL56489), and some bacterial species (ZP_01170511.1 of *Bacillus* sp., NP_563502 of *Clostridium perfringens*, and NP_350006 of *Clostridium acetobutylicum*; data not shown). An EST clone (AV618908) in *Chlamydomonas reinhardtii* and several ribonuclease II family proteins in some *Cyanobacteria* species, showing very low similarities to AtNYE1 though, were also revealed in the *C. reinhardtii* ESTs and *Cyanobacteria* databases (http://www.kazusa.or.jp/en/plant/database.html). Even though highly conserved among higher plants, domain sequences hardly provide any cues about its possible biochemical roles. However, a variety of potential modifications are suggested by the presence of three *N*-glycosylation sites, four protein kinase C phosphorylation sites, three casein kinase II phosphorylation sites, and an *N*-myristoylation site (Bairoch et al., 1997).

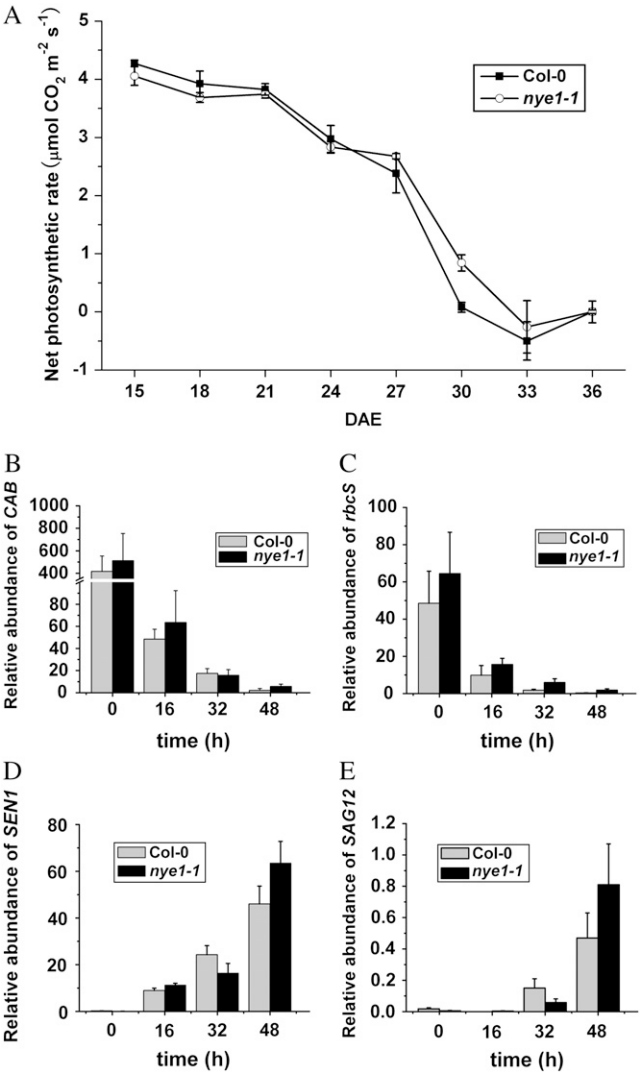

Figure 6. Photosynthetic capacity and senescence-associated processes in *nye1-1*. A, Changes of the net photosynthetic rate in the fourth rosette leaves of *nye1-1* and Col-0. Error bars indicate SD, $n = 5$. B to E, Changes in the transcript levels of four well characterized photosynthesis- or senescence-associated genes during a 48-h dark incubation. B to E present the data of *CAB*, *RBCS*, *SEN1*, and *SAG12* transcripts, respectively. Transcript levels quantified by real-time RT-PCR, *ACTIN2* as the reference. Values are means of three replicates. Error bars indicate SD. The experiments were repeated once.

Twelve sequences from eight representative plant species, corresponding to the amino acids between 78 and 211 in AtNYE1, were adopted to construct a phylogenetic tree (Fig. 10B). The angiosperms-gymnosperms divergence and monocot-dicot divergence were well reflected on the tree. Furthermore, our data also suggest that the divergence of family members within a species is posterior to the divergence of species.

AtNYE1 Localized in Chloroplast

To verify the prediction that AtNYE1 was likely targeted to the chloroplast, its C terminus was fused to enhanced yellow fluorescent protein (eYFP) and the resultant fusion protein was introduced into *nye1-1*. Transgenic plants expressing the AtNYE1-eYFP fusion protein driven by the 35S promoter also could result in albino seedlings or pale-yellow true leaves (data not shown), suggesting that the AtNYE1-eYFP fusion protein was functioning properly. Expectedly, eYFP fluorescence in albino seedlings was predominantly observed in chloroplast (Fig. 11), while it was hardly detected in those phenotypically normal transgenic plants (data not shown). By comparison, eYFP in the 35S-*eYFP* control plants was present in both cytoplasm and nucleus (Fig. 11). These data confirm that AtNYE1 is localized in chloroplast.

Spatial and Temporal Transcriptions of *AtNYE1*

In attempt to elucidate its physiological function in Arabidopsis, relative transcriptions of *AtNYE1* in different organs and in leaves at various developmental stages were determined by real-time PCR. The transcript of *AtNYE1* was detected in all the organs examined, with relatively higher levels being detected in flowers and buds, medium to low levels in siliques, and the lowest in roots, seedlings, and young rosette leaves (Fig. 12A). As expected, *AtNYE1* was strongly induced by dark treatment or natural senescence (Fig. 12, B and C; Guo et al., 2004; Armstead et al., 2006). Interestingly, in *nye1-1*, its expression was also sharply induced, as it was in Col-0, by dark treatment (Fig. 12C).

DISCUSSION

NYE1 Is a Key Regulator Directly Associated with Chl Degradation during Organ Senescence or Maturation

Recent studies showed that alterations in the sequences of *AtNYE1* orthologs were associated with stay-green phenotypes in various crop species. In rice, a missense mutation was identified in its putative ortholog (*SGR*) through mapping a stay-green locus (Cha et al., 2002; Hörtensteiner, 2006). In *F. pratensis*, a

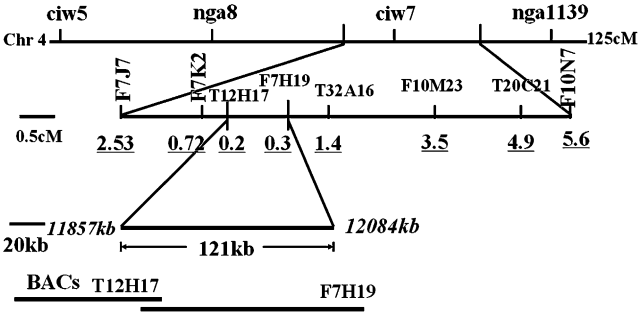

Figure 7. Mapping of *AtNYE1* locus. Numerals in bold and underlined indicate the rates of recombinants, and ones in italic indicate physical distances (kb). Chr. 4, Chromosome 4; cM, centimorgan; BACs, bacterial artificial chromosomes.

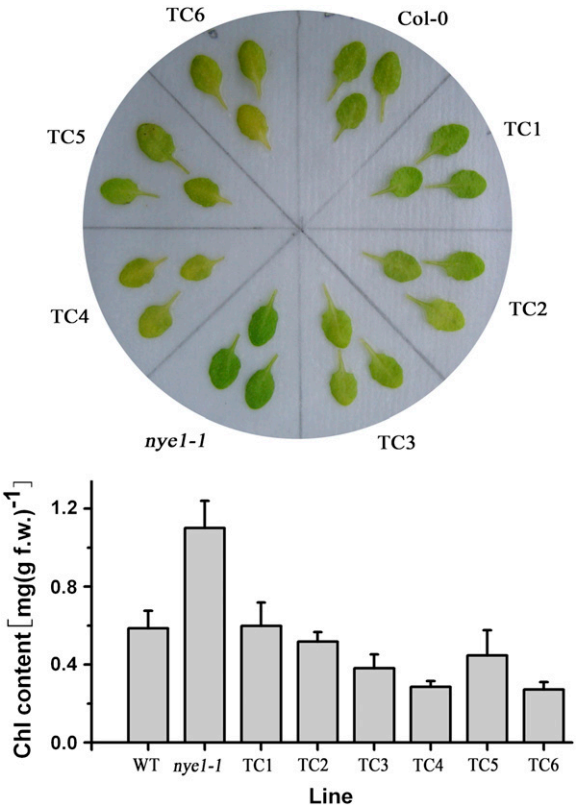

Figure 8. Complementation of *nye1-1* phenotype by a 4.1 kb genomic DNA fragment containing *AtNYE1*. A, Phenotypes of T2 complemented lines, Col-0, and *nye1-1* leaves after a 4-d incubation in darkness. TC1 to TC6 represents six independent lines. B, A graph displaying total Chl content of leaf tissues depicted in A. Values are means of three replicates. Error bars indicate SD. [See online article for color version of this figure.]

four-base (ATAT) insertion in its putative ortholog (*Y*) was also reported to be genetically associated with the stay-green phenotype of the most extensively analyzed nonyellowing mutant, Bf993 (Thomas and Stoddart, 1975; Thomas et al., 1999; Roca et al., 2004; Armstead et al., 2006). Even more amazingly, the color (yellow versus green) trait of cotyledons in pea (*Pisum sativum*), first described by Mendel in 1866, was recently considered to be due to a variation in intron size of its putative ortholog (*I*; Armstead et al., 2007). However, the function of these orthologs has not been confirmed by genetic complementation in any of these crops, probably due to their recalcitrance to genetic transformation. In this study, *AtNYE1* genomic copy can rescue the *nye1-1* phenotype in more than 10 independent transformants, confirming that the *NYE1* encodes the gene responsible for the nonyellowing phenotype. These data collectively indicate that NYE1 may play a key role in regulating Chl degradation during senescence in plants.

RNA interference and overexpression have been adopted to analyze the regulatory role of *AtNYE1* on Chl degradation in Arabidopsis. In RNA interference plants, Chl degradation was delayed significantly during dark-induced senescence (L. Yang and B. Kuai, unpublished data; Armstead et al., 2007). Strong up-regulation of *AtNYE1* expression can result in either pale-yellow true leaves or albino seedlings, while slight up-regulation of its expression causes no significant changes in the phenotype (Fig. 9). These results, along with the semidominant nature, or haploinsufficiency, of the mutation, clearly indicate that the *NYE1* transcript abundance is closely correlated with an effect on Chl degradation. Practically, this correlation implies that a regulatory effect on Chl catabolism could be imposed by modulating *NYE1* transcript level.

In a series of related studies, Chl degradation is also found to be affected by plant hormones, such as cytokinin and ethylene. However, this kind of effect is mainly considered an indirect consequence of altered senescence (Smart, 1994; Gan and Amasino, 1995). In *nye1-1*, both photosynthetic capacity/process and senescence process are not significantly affected, indicating that Chl degradation is directly slowed down by the null mutation of *AtNYE1*. It is therefore fairly convincing to conclude that *NYE1* directly regulates Chl degradation during organ senescence or maturation, and the identification of *nye1-1* mutant in

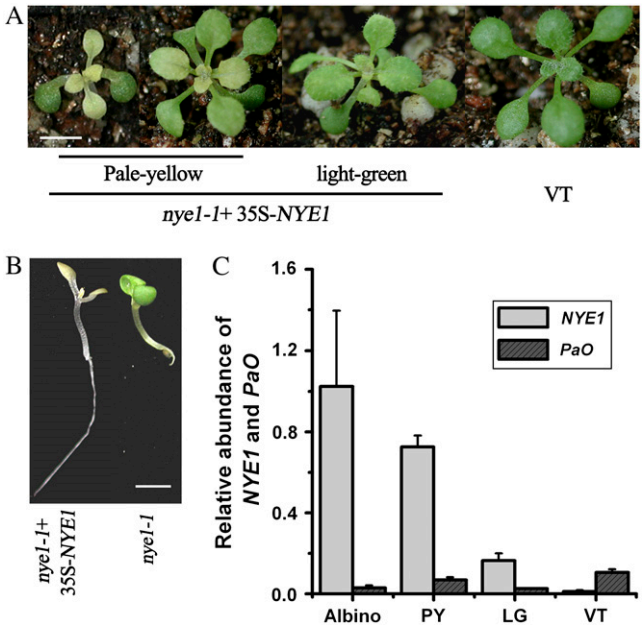

Figure 9. Phenotypes of the *nye1-1* mutants transformed with 35S-*AtNYE1*. A, Morphology of three representative T1 transgenic plants with a different shade of yellowish phenotype. Bar = 0.5 cm. VT, *nye1-1* transformed with pCHF3 control vector. B, Albino seedlings and *nye1-1* grown on one-half Murashige and Skoog medium containing 2% Suc and 50 mg L^{-1} kanamycin for 13 d under short-day condition (8-h light/16-h dark). Bar = 0.5 cm. C, qPCR analysis of the expression of *NYE1* and *PaO*, with *ACTIN2* as the reference. Values are means of three replicates. Error bars indicate SD. Albino, Albino transformants; PY, pale-yellow; LG, light-green. qPCR was repeated once with similar results. [See online article for color version of this figure.]

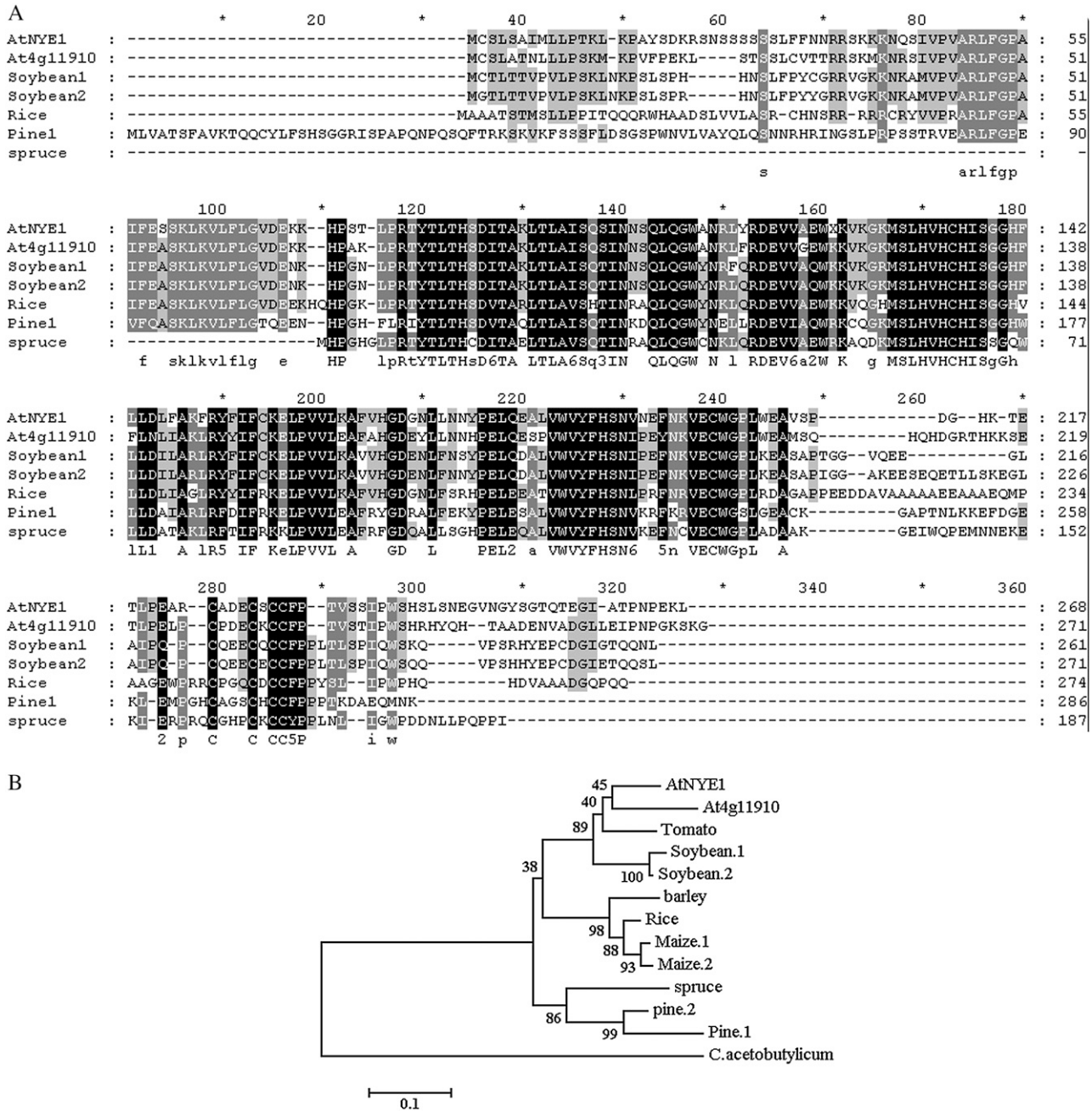

Figure 10. Evolutionary conservation of AtNYE1 among diversified plants species. A, An alignment of predicted amino acid sequences of AtNYE1 putative paralogs and orthologs from Arabidopsis, soybean (*Glycine max*), rice, pine (*Pinus* spp.), and spruce (*Picea abies*). Residues conserved across all 10 species are shaded black; residues conserved across six to nine species are shaded gray. Consensus sequences are shown underneath; conserved groups are as follows from top to bottom: 1 = DN, 2 = EQ, 3 = ST (hydroxylated), 4 = KR (basic), 5 = FYW (aromatic), and 6 = LIVM (aliphatic or M). Sequences were aligned by the ClustalX software and displayed by the GenDoc program (Nicholas et al., 1997). B, Phylogenetic analysis of putative NYE1 paralogs and orthologs using MEGA with neighbor-joining method, bootstrap analysis was performed with 1,000 replicates and excluding positions with gaps. Numbers in branches indicate bootstrap values (percent). *C. acetobutylicum* (AAK81346) is employed as an outlier. Tomato (*Solanum lycopersicum*; accession no. AY98500), soybean1 (AAW82959), soybean2 (AAW82960), rice (AY850134), barley (*Hordeum vulgare*; AAW82955), maize1 (*Zea mays*; AAW82956), maize2 (AAW82957), spruce (TC identifier TC2485), pine1 (*Pinus teada*; TC73170), and pine2 (TC72969).

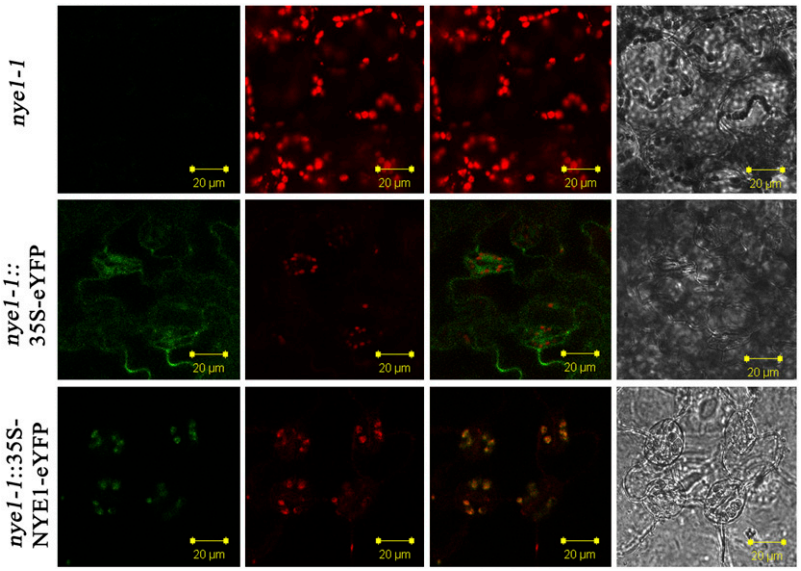

Figure 11. Localization of AtNYE1 in chloroplast. Micrographs of leaf tissue from *nye1-1* (top), *nye1-1* expressing the 35S-*eYFP* reporter (middle), and *nye1-1* expressing the 35S-*AtNYE1-eYFP* reporter (bottom). First column: confocal micrographs of fluorescence from eYFP (green channel). Second column: Chl autofluorescence (red channel). Third column: merged micrographs of red and green images. Fourth column: transmitted light image. Of each construct, three or more independent lines were taken for observation. Bar = 20 μm.

Arabidopsis opens wide possibilities for exploring the genetic and molecular regulatory mechanisms of Chl degradation.

NYE1 Accelerates Chl Degradation by Maintaining Sufficient PaO Activity

Although highly conserved domains are present in its putative orthologs of various plant species, no informative implications about the molecular and biochemical roles of NYE1 have been revealed by any of the available bioinformatical analyses. Nevertheless, experimentally examining (chemical, biochemical, and molecular) parameters associated to green pigment (Chl, Chlide, and Pheide) breakdown in *nye1-1* demonstrated that PaO activity was greatly reduced, with an estimated reduction of about 50% to approximately 80%. This detection is in accordance with that observed in Bf993 of *F. pratensis* (Vicentini et al., 1995), which provides further evidence to the postulation that the four-base insertion in the *NYE1* ortholog might be responsible for the stay-green phenotype (Armstead et al., 2006). The reduction of PaO activity in these *NYE1* mutants indicates that NYE1 normally accelerates Chl degradation during senescence by maintaining sufficient PaO activity to ensure no accumulation of the photodynamic Pheide *a*. One of the immediate speculations is that NYE1 might directly or indirectly interact with PaO or a complex of enzymes involving PaO (for a recent review, see Hörtensteiner, 2006). This hypothesis is supported by the fact that the expression of *PaO* was not affected in *nye1-1* (Fig. 4B), implying that the modulation likely occurs at the protein level. This implication is consistent with recent findings that the PaO activity might be posttranslationally regulated, mainly through PaO dephosphorylation (Chung et al., 2006). Interestingly, the expression of *PaO* was not found to be induced in albino seedlings expressing 35S-*AtNYE1*, which might imply that NYE1 plays a dual role in both initiating Chl degradation and modulating the residual PaO activity that appears to be sufficient for the degradation of Pheide *a*.

On the other hand, Chl in *NYE1* mutants was still being degraded upon dark incubation, even in the null

Table II. *Newly designed SSLP primer sets*
BAC, Bacterial artificial chromosome.

Marker	BAC	Position on Chromosome		Oligonucleotide Sequences		PCR Product Size	
				Forward Primer	Reverse Primer	Col-0	*Ler*
		bp				*bp*	
AtF10M23	F10M23	13,497,140	13,497,150	5′AGAGTGGTGGATAGGAGGAC3′	5′AGTTATGTTCAAATCTGTCGTT3′	169	153
AtF7J7	F7J7	11,293,794	11,293,810	5′TTGATGATTCCCTTGTTTGA3′	5′TAGTGGCTGAAAAGGAGAAA3′	149	134
AtF7K2	F7K2	11,857,443	11,857,462	5′ACCAAATGCCTACCACAA3″	5′ATGTATTTTTTGCCTTTTCC3′	165	147
AtT12H17	T12H17	11,953,277	11,953,289	5′ATAACAACCCACTCACACAA3′	5′AAATCGTTTCTTATCCTTCC3′	150	137
AtF7H19	F7H19	12,107,952	12,107,971	5′CAATGGAAGGCTATTTGTCTA3′	5′ACTCAGATAGAGAAATTAGGTGATA3′	139	121
AtT32A16	T32A16	12,459,190	12,459,221	5′TAAAGGAAAATGGACCTAACTA3′	5′CTTGTTTGGTTTTGAGGTTC3′	213	183

mutant *nye1-1*, indicating that there might exist a paralog, less efficient though, of NYE1, or even an alternative Chl degradation pathway. Our HPLC analysis data, along with Roca's (Roca et al., 2004), seemingly supports the assumed existence of a less efficient paralog, which is presumably also less competent in occupying a putative acting site. In Bf993, Chlide *a* and Pheide *a* were found to accumulate sequentially, with the Chlide *a* accumulation being much more significant; in *nye1-1*, however, no detectable levels of such catabolites were accumulated, although a similar changing pattern in the dynamics of Chl degradation was observed (Thomas, 1987; Thomas et al., 1999). These observations indicated that the Chl degradation pathway in Bf993 suffered a more dramatic interference than that in *nye1-1*. However, according to Armstead's report (Armstead et al., 2006), a four-base insertion in the *NYE1* ortholog in Bf993 resulted in a final protein consisting of 232 residues, with its amino acid sequence from position 100 being radically changed; whereas the nonsense mutation in *AtNYE1* in *nye1-1* caused an early termination of translation, which results *nye1-1* as a null mutant. Only when a paralog, not only less efficient but also less competitive in occupying a putative acting site is assumed to exist, could these data be plausibly explained, i.e. the truncated protein in Bf993 was even less efficient in functioning but still more competitive in occupying a putative acting site than its wild-type paralog, while, *in nye1-1*, the wild-type paralog was functioning properly, presumably without being subject to such a competition. It has been indicated that the formation of pFCC-1 from Pheide *a* requires an unknown factor, RFF, which is present in *Escherichia coli* (Pružinská et al., 2005). Since no NYE1 homologs are found in *E. coli*, it can be excluded that NYE1 is identical with RFF. In Arabidopsis, at4g11910 could be a candidate paralog. However, both the genetic role of at4g11910 and the molecular nature of RFF have not been revealed.

NYE1 Likely Promotes Higher Plant Growth and Development by Timely Remobilizing Nitrogen Nutrition from Senescing Organs to Nascent Ones

It has been reported that the growth and productivity of stay-green plants of *Lolium prenne*, with the putative *NYE1* mutant ortholog introgressed from Bf993, are significantly reduced compared to wild-type plants under conditions of extreme nitrogen (N) limitation, and the extra retention of leaf N in its senescing leaves contributes a functionally significant proportion of the total N content of the plant with respect to growth potential (Macduff et al., 2002). In this study, although no experiments were deliberately designed to precisely examine the N nutrition remobilization, a significant 9-d delay in bolting and consequently flowering was observed in *nye1-1* relative to that in the wild type, both of which were grown under standard Arabidopsis growth conditions, without applying nutrition after vegetative growth, a condition similar to N limitation at the later stages. An immediate significance of this coincidence in inhibition to plant growth and development would not only reinforce the speculation that *Sid*, or recently redesignated as *Y* in *F. pratensis*, was the ortholog of *AtNYE1*, but more importantly, also imply that NYE1 has been likely evolved as a promoter of higher plant growth and development by timely remobilizing N nutrition from senescing organs to nascent ones. This implication is evidenced by the fact that the putative orthologs of NYE1 predominantly appear in higher plant species, multigreen organs of which develop and senesce sequentially.

In conclusion, NYE1 has been convincingly identified as a key and direct regulator of Chl degradation during senescence, probably by modulating PaO activity. The successful identification of *NYE1* mutation in Arabidopsis would not only provide an efficient system to analyze its molecular and biochemical roles, but also greatly facilitate further exploration for the regulatory mechanism of Chl degradation in general.

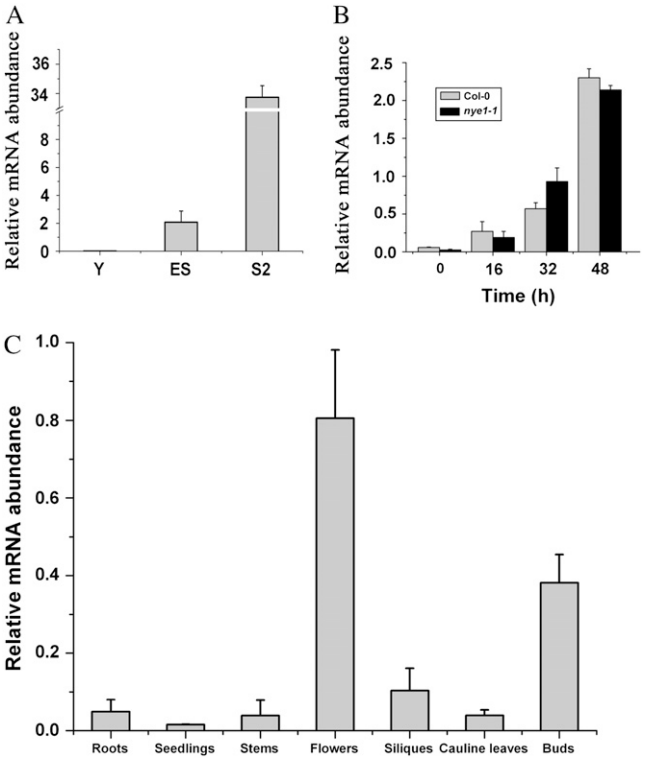

Figure 12. Temporal and spatial expression patterns of *AtNYE1*. A, Spatial expression pattern of *AtNYE1* in the wild type. B, *AtNYE1* transcript levels in the leaves of different developmental stages in the wild type. Y, Young leaves; ES, early senescence; S2, progressive senescence stage 2 (Gepstein et al., 2003). C, Changes in *AtNYE1* transcript levels during a 48-h incubation in darkness in Col-0 and *nye1-1*. cDNA abundances quantified by real-time RT-PCR, *ACTIN2* as the reference. Values are means of three replicates. Error bars indicate SD. The experiment was repeated once.

MATERIALS AND METHODS

Plant Materials and Growth Conditions

All the wild-type and mutant Arabidopsis (*Arabidopsis thaliana*) lines used in this study are in the Col-0 background unless indicated otherwise. Seeds were sown in square pots (10 cm in length) with soil (v [peat soil]:v [vermiculite]:v [pearlite] = 3:9:0.5; Shanghai Institute of Landscape Science) presoaked with plant nutrient medium including 0.5% Suc (Estelle and Somerville, 1987). Plants were grown at 24°C, with an approximately 100 μmol m^{-2} s^{-1} light intensity under a 16-h light /8-h dark photoperiod.

For dark treatment, leaves 4 to 6, or whole plants without roots, from 3- to 4-week-old Arabidopsis plants were excised and incubated on wet filter paper in total darkness at 25°C for various periods, as indicated. For the dark treatment of whole plants in soil, trays were covered with black bags and incubated in growth room for a period of time as indicated.

Mutant Screening

The fast-neutron mutagenized M2 seeds in Col-0 genetic background were purchased from Lehle Seeds (Round Rock). About 50,000 3-week-old M2 plants were incubated in darkness for 6 d to screen mutants with delayed Chl loss. The putative screened mutants were subjected to further confirmation for a couple of times during the remaining growth period by visually checking the phenotypes of their detached leaves incubated in permanent darkness for 4 to 6 d. A stable nonyellowing mutant, without obvious pleiotropic effects, was finally identified and designated as *nye1-1*. It was then backcrossed with the wild-type Col-0 four times, and the resulting homozygous *nye1-1* plants were used for further analysis.

Map-Based Cloning

For genetic analysis of the mutation, *nye1-1* plants were crossed with the wild-type Col-0 as well as L*er* plants reciprocally, and the resulting F1 seedlings were allowed to self-pollinate to produce F2 populations. Phenotypes of F1 and F2 were visually classified and scored as mutant, intermediate, or wild type.

Mapping procedure was performed as described by Lukowitz and Jander (Lukowitz et al., 2000; Jander et al., 2002). From the F2 population of a cross between *nye1-1* and wild-type L*er* plants, 828 plants showing mutant phenotype were selected to construct a mapping population. The homozygosity of the selected plants was checked in F_3 generations. *NYE1* locus was initially mapped using 22 SSLP markers (selected from the Arabidopsis Information Resource, http://www.arabidopsis.org/) with a mixed sample of DNAs extracted from 100 selected plants individually. The interval was narrowed down with newly designed markers (Table II). The candidate gene was identified by sequencing ORFs of putative genes within the expected region. PCR amplifications were performed using Primerstar DNA polymerase (TaKaRa Biotechnology).

Plasmid Construction

For the genomic complementation test, a 4.1-kb DNA fragment containing the predicted ORF as well as 1.9 kb promoter region and 1.0 kb downstream sequence was amplified from the wild type by PCR using two oligonucleotides, 5′ CACGGATCCAACAAGATCTAACCCTTTTG 3′ and 5′ CAGCTGCAGTGGAGGTGACAGGAGG 3′ (the lowercase c is an introduced mismatch to create restriction site, underlined). The fragment was subcloned into *Pst*I and *Bam*HI sites of pPZP221 (Hajdukiewicz et al., 1994) and sequenced with self-designed primers (data not shown).

For subcellular localization test, the *eYFP* coding region (Ge et al., 2005) was amplified with two primers: 5′ CATGATATCATGGTGAGCAAGGGCGAGGAGC 3′ (the underlined sequence is an *Eco*RV site) and 5′ CATGAGCTCTTACTTGTACAGCTCGTCCATG 3′ (the underlined sequence is a *Sac*I site). The *AtNYE1* coding sequence was amplified from Col-0 genomic DNA with 5′ CATGGATCCATGTGTAGTTTGTCGGCGATTA 3′ (the underlined sequence is a *Bam*HI site) and 5′ CATGATATCGAGTTTCTCCGGATTTGGAGTA 3′ (the underlined sequence is an *Eco*RV site). The PCR products were cloned into pMD19-T vector (TaKaRa Biotechnology) and sequenced. After digestion, the released fragments were subcloned into pPZPY122 (Hajdukiewicz et al., 1994).

For overexpression of *AtNYE1*, the full-length coding region (807 bp) was amplified with a pair of primers 5′ CATGGTACCATGTGTAGTTTGTCGGCGATTATG 3′ (the underlined sequence is a *Kpn*I site) and 5′ CATGGATCCCTAGAGTTTCTCCGGATTTGGAG 3′ (the underlined sequence is a *Bam*HI site). The PCR products were cloned into pMD 19-T vector and sequenced. After digesting with *Kpn*I and *Bam*HI, the releasing fragment was subcloned into pCHF3 binary vector (Ge et al., 2005).

Plant Transformation

The above constructs were introduced into the *Agrobacterium tumefaciens* strain LBA4404. Plants were transformed via the floral-dipping method (Clough and Bent, 1998). Putative transgenic plants were initially selected with 90 mg L^{-1} Gentamycin (for pPZP221 derived constructs and pPZPY122 derived constructs) or 50 mg L^{-1} Kanamycin (for pCHF3 derived contructs), and their transgenic status was determined by PCR analysis.

Fluorescence Microscopy

Excised leaves were mounted on glass with a drop of water and then covered with coverslips. They were examined by confocal microscopy using a LSM 510 laser scanning confocal microscope (ZEISS) with a 40× oil immersion objective. Chl autofluorescence and YFP signal were sequentially excited by switching between the 488- and 514-nm laser lines, respectively. The fluorescence emission was selected by a band pass filter (BP530–600) for eYFP and a long pass filter (LP560) for Chl fluorescence. Recorded images from the microscopes were processed with Adobe Photoshop (Adobe Systems).

Real-Time Reverse Transcription-PCR

Total RNA was extracted from control and dark-treated leaves of Col-0 using Trizol Reagent (Invitrogen), followed by chloroform extraction, isopropanol precipitation, and spectrophotometric quantification. After digestion with Rnase-free DNase (Promega), 2 μg total RNA was reverse transcribed with the Superscript reverse transcriptase (Shenenergy Biocolor). The products were subsequently used as templates for real-time PCR analysis. The real-time PCR was performed using SYBR Green I PCR kit (Toyobo) on an iCycler according to the manufacturer's suggestions, with *ACT2* as a reference (Bio-Rad).

Specific primers to respective genes were as follows: *ACT2* (forward, 5′-CGCTCTTTCTTTCCAAGCTC-3′ and reverse, 5′-AACAGCCCTGGGAGCATC-3′); *AtNYE1* (forward, 5′-GCAAGGATGGGCAAATAGG-3′ and reverse, 5′-CACCGCTTATGTGACAATGAAC-3′); *SAG12* (forward, 5′-TGGATACGGCGAATCTACTAACG-3′ and reverse, 5′- GCTTTCATGGCAAGACCACATAG-3′); *SEN1* (forward, 5′-GTCATCGGCTATTTCTCCACCT-3′ and reverse, 5′-GTTGTCGTTGCTTTCCTCCATC-3′); *CAB* (forward, 5′-CCAGAGGCATTCGCTGAGTTG-3′ and reverse, 5′-CCTTACCAGTGACGATGGCTTG-3′); *RBCS* (forward, 5′-CCACCCGCAAGGCTAACAAC-3′ and reverse, 5′-TTCGGAATCGGTAAGGTCAGG-3′); *PaO* (forward, 5′-GAAAATGGTTGGGATAGAGC-3′ and reverse, 5′-TGGGTTGGAGTGAATGTGAG-3′); *ATCLH1* (forward, 5′-GGCATCGGAAAACCTCAA-3′ and reverse, 5′-ATCTCCGCTTTTTCACCC-3′); *RCCR* (forward, 5′-CATGGAAGACCACGACGATCA-3′ and reverse, 5′-GGAGGGAGGTTACAGGGAAGG-3′).

Photosynthetic Rate Measurement

Net photosynthetic rate was measured using LI-6400 (LI-COR) under a fixed LED light source (500 μmol m^{-2} s^{-1}) at 25°C, as described in the manufacturer's instruction.

Measurement of Chl Contents and Detection of Its Catabolites

For pigment quantification, leaves 4 to 6 (about 0.1 g fresh weight) from 3- to 4-week-old plants were taken. After dark treatment, excised leaves were immediately frozen in liquid N and stored at −80°C. Chl contents were quantified by spectrometer according to Benedetti and Arruda (Benedetti and Arruda, 2002), and HPLC analysis was performed on Aglient 1100 HPLC by using Almela's method at 440 nm (Almela et al., 2000). Identification of pigments was based on their respective retention time or coinjection with standard pigment.

Standard Chl *a* was purchased from Sigma and Pheide *a* from Wako Chemicals. Chlide *a* was prepared by digesting Chl *a* with Chlase, as described

by Fang (Fang et al., 1998), and verified by its spectral pattern. To further verify the preparation, the prepared Chlide *a* was acidified with HCl to remove Mg, and the resultant Pheide *a* was confirmed by referring to the retention time of standard Pheide *a*. Chl *b* was prepared by the following procedure under darkness at 4°C. Chls were first extracted and partially purified from spinach (*Spinacia oleracea*) leaves according to a reported protocol (Iriyama et al., 1974). Suc was ground into fine powder and roasted at 70°C for 2 h. It was then loaded into a column with petroleum ether after being cooled down to room temperature. The purified Chls were then dissolved in petroleum ether and transferred into the column. After xanthin was eluted by petroleum ether, petroleum ether/acetone/benzene (20/2/1, v/v/v) was used to separate the remaining compounds. Chl *b*, showing a yellow-green color, was then collected, dried, and redissolved in acetone.

Chlase Assay

Chlase activity was measured according to a reported protocol (Todorov et al., 2003), with an exception that acetone power was dried and weighed. Chlase activity data were normalized to total protein content, determined by bicinchoninic acid method (Smith et al., 1985), and the total protein content was normalized to dry acetone powder weight.

PaO Assays

PaO was measured using a coupled assay with RCCR according to previous reports, with a slight modification (Hörtensteiner et al., 1995; Vicentini et al., 1995). Briefly, leaf samples were homogenized in 5 mL/g fresh weight of a medium containing 400 mM sorbitol, 25 mM Tricine-KOH, pH 8.0, 2 mM EDTA, 1 mM $MgCl_2$, 0.1% bovine serum albumin (w/v), 5 mM polyethylene glycol 4,000, and 0.5 mM dithiothreitol, with chilled mortars and pestles. After filtration through two layers of cloth, the homogenate was centrifuged at 7,000*g* for 4 min. The green sediment was washed once with buffered medium (the above medium with EDTA, $MgCl_2$, and polyethylene glycol 4,000 omitted). After centrifugation at 8,000*g* for 5 min, pellets were resuspended in the same buffered medium (2 mL/g fresh weight leaf tissue) and 1 mL aliquots were pipetted into 1.5 mL tubes. After centrifugation at 14,000*g* for 5 min, sediment in the tube was frozen in liquid N and stored at −80°C.

The PaO and RCCR were prepared strictly according to the previous protocols. Soluble stroma protein (S1 fraction) was used as the source of RCCR and solubilized membrane protein in osmotic buffer (Tris-MES, pH 8.0, 0.1% bovine serum albumin) with 1% Triton X-100 used as the source of PaO.

For PaO assay, the reaction mixture (50 μL) contained Pheide *a* (30 μg) as substrate and the ferredoxin-reduced system as cofactors: 10 μg ferredoxin (Sigma), 1 mM NADPH (Sigma), 1 mM Glc-6-P (G6P), and 10 milliunits of G6P dehydrogenase. After incubation in the dark at 25°C for 1 h, the reaction was terminated with methanol at a final concentration of 70%. After centrifugation at 14,000*g* for 10 min, the supernatant was analyzed for pFCC-1 by reverse-phase HPLC with 0.1 M potassium phosphate (pH 7.0)/methanol (32.5%: 67.5%, V/V).

HPLC analyses were performed with a Waters 2690 HPLC coupled to a Waters 2475 fluorescence detector equipped with a ZorbaxSB C-18 column (4.6 mm × 25 cm, 5-μm particle diameter). Twenty microliters were injected at a flow rate of 0.8 mL/min. Under these conditions, pFCC-1 was eluted after 5.8 min. Fluorescence was recorded at 320 nm (excitation)/450 nm (emission). The amount of pFCC-1 was given as integrated peak areas.

Accession Numbers

The GenBank accession numbers for *AtNYE1* and At4g11910 are DQ437531 and DQ437532, respectively.

Supplemental Data

The following materials are available in the online version of this article.

Supplemental Figure S1. Nonyellowing phenotype of *nye1-1* siliques.

ACKNOWLEDGMENTS

Mutant screening was conducted at Dong Lab, Developmental, Cell and Molecular Biology group, Department of Biology, Duke University. We are grateful to Profs. X. Dong and H. Huang for their valuable advice and help. We would also like to thank Profs. J. Huang and H. Mi for the gifts of G6P and G6P dehydrogenase, Dr. T. Zhou, Mr. C. He, and Miss Z. Huang for their help in HPLC analysis, Profs. Z. Yang and Mr. Q. Shi for their help in microscopy, and Dr. L. Jiang for her help in photosynthetic rate measurement.

Received March 25, 2007; accepted April 23, 2007; published April 27, 2007.

LITERATURE CITED

Akhtar MS, Goldschmidt EE, John I, Rodoni S, Matile P, Grierson D (1999) Altered patterns of senescence and ripening in *gf*, a stay-green mutant of tomato (*Lycopersicon esculentum* Mill.). J Exp Bot **50:** 1115–1122

Almela L, Fernandez-Lopez JA, Roca MJ (2000) High-performance liquid chromatographic screening of chlorophyll derivatives produced during fruit storage. J Chromatogr A **870:** 483–489

Armstead I, Donnison I, Aubry S, Harper J, Hörtensteiner S, James C, Mani J, Moffet M, Ougham H, Roberts L, et al (2006) From crop to model to crop: identifying the genetic basis of the staygreen mutation in the *Lolium/Festuca* forage and amenity grasses. New Phytol **172:** 592–597

Armstead I, Donnison I, Aubry S, Harper J, Hörtensteiner S, James C, Mani J, Moffet M, Ougham H, Roberts L, et al (2007) Cross-species identification of Mendel's *I* locus. Science **315:** 73

Bairoch A, Bucher P, Hofmann K (1997) The PROSITE database, its status in 1997. Nucleic Acids Res **25:** 217–221

Benedetti CE, Arruda P (2002) Altering the expression of the chlorophyllase gene *ATHCOR1* in transgenic Arabidopsis caused changes in the chlorophyll-to-chlorophyllide ratio. Plant Physiol **128:** 1255–1263

Cha KW, Lee YJ, Koh HJ, Lee BM, Nam YW, Paek NC (2002) Isolation, characterization, and mapping of the stay green mutant in rice. Theor Appl Genet **104:** 526–532

Chung DW, Pružinská A, Hörtensteiner S, Ort DR (2006) The role of pheophorbide *a* oxygenase expression and activity in the canola green seed problem. Plant Physiol **142:** 88–97

Clough SJ, Bent AF (1998) Floral dip: a simplified method for Agrobacterium-mediated transformation of *Arabidopsis thaliana*. Plant J **16:** 735–743

Efrati A, Eyal Y, Paran I (2005) Molecular mapping of the chlorophyll retainer (*cl*) mutation in pepper (*Capsicum* spp.) and screening for candidate genes using tomato ESTs homologous to structural genes of the chlorophyll catabolism pathway. Genome **48:** 347–351

Emanuelsson O, Nielsen H, Von Heijne G (1999) ChloroP, a neural network-based method for predicting chloroplast transit peptides and their cleavage sites. Protein Sci **8:** 978–984

Estelle MA, Somerville CR (1987) Auxin-resistant mutants of *Arabidopsis thaliana* with an altered morphology. Mol Gen Genet **206:** 200–206

Fang ZY, Bouwkamp JC, Solomos T (1998) Chlorophyllase activities and chlorophyll degradation during leaf senescence in non-yellowing mutant and wild type of *Phaseolus vulgaris L.* J Exp Bot **49:** 503–510

Gan S, Amasino RM (1995) Inhibition of leaf senescence by autoregulated production of cytokinin. Science **270:** 1986–1988

Ge X, Dietrich C, Matsuno M, Li G, Berg H, Xia Y (2005) An Arabidopsis aspartic protease functions as an anti-cell-death component in reproduction and embryogenesis. EMBO Rep **6:** 282–288

Gepstein S, Sabehi G, Carp MJ, Hajouj T, Nesher MFO, Yariv I, Dor C, Bassani M (2003) Large-scale identification of leaf senescence-associated genes. Plant J **36:** 629–642

Gray J, Close PS, Briggs SP, Johal GS (1997) A novel suppressor of cell death in plants encoded by the Lls1 gene of maize. Cell **89:** 25–31

Guiamét JJ, Teeri JA, Noodén LD (1990) Effects of nuclear and cytoplasmic genes altering chlorophyll loss on gas-exchange during monocarpic senescence in soybean. Plant Cell Physiol **31:** 1123–1130

Guiamét JJ, Tyystjarvi E, Tyystjarvi T, John I, Kairavuo M, Pichersky E, Noodén LD (2002) Photoinhibition and loss of photosystem II reaction centre proteins during senescence of soybean leaves: enhancement of photoinhibition by the ''stay-green'' mutation *cytG*. Physiol Plant **115:** 468–478

Guo Y, Cai Z, Gan S (2004) Transcriptome of Arabidopsis leaf senescence. Plant Cell Environ **27:** 521–549

Hajdukiewicz P, Svab Z, Maliga P (1994) The small, versatile ppzp family of Agrobacterium binary vectors for plant transformation. Plant Mol Biol **25:** 989–994

Hörtensteiner S (2006) Chlorophyll degradation during senescence. Annu Rev Plant Biol **57:** 55–57

Hörtensteiner S, Vicentini F, Matile P (1995) Chlorophyll breakdown in senescent cotyledons of rape, brassica-napus L—enzymatic cleavage of Phaeophorbide-*a in-vitro*. New Phytol **129:** 237–246

Iriyama K, Ogura N, Takamiya A (1974) A simple method for extraction and partial purification of chlorophyll from plant material, using dioxane. J Biochem (Tokyo) **76:** 901–904

Jacob-Wilk D, Holland D, Goldschmidt EE, Riov J, Eyal Y (1999) Chlorophyll breakdown by chlorophyllase: isolation and functional expression of the *Chlase1* gene from ethylene-treated *Citrus* fruit and its regulation during development. Plant J **20:** 653–661

Jander G, Norris SR, Rounsley SD, Bush DF, Levin IM, Last RL (2002) Arabidopsis map-based cloning in the post-genome era. Plant Physiol **129:** 440–450

Lukowitz W, Gillmor CS, Scheible WR (2000) Positional cloning in Arabidopsis: why it feels good to have a genome initiative working for you. Plant Physiol **123:** 795–805

Luquez VM, Guiamét JJ (2002) The stay green mutations *d1* and *d2* increase water stress susceptibility in soybeans. J Exp Bot **53:** 1421–1428

Macduff J, Raistrick N, Humphreys M (2002) Differences in growth and nitrogen productivity between a stay-green genotype and a wild-type of *Lolium perenne* under limiting relative addition rates of nitrate supply. Physiol Plant **116:** 52–61

Nicholas KB, Nicholas HB Jr, Deerfield DW II (1997) GeneDoc: analysis and visualization of genetic variation. EMBnet.news **4:** 1–4

Oh MH, Kim JH, Moon YH, Lee CH (2004) Defects in a proteolytic step of light harvesting complex II in an Arabidopsis stay-green mutant, *ore10*, during dark-induced leaf senescence. J Plant Biol **47:** 330–337

Oh MH, Moon YH, Lee CH (2003) Increased stability of LHCII by aggregate formation during dark-induced leaf senescence in the Arabidopsis mutant, *ore10*. Plant Cell Physiol **44:** 1368–1377

Pružinská A, Tanner G, Anders I, Roca M, Hörtensteiner S (2003) Chlorophyll breakdown: pheophorbide *a* oxygenase is a rieske-type iron-sulfur protein, encoded by the *accelerated cell death 1* gene. Proc Natl Acad Sci USA **100:** 15259–15264

Pružinská A, Tanner G, Aubry S, Anders I, Moser S, Muller T, Ongania KH, Kräutler B, Youn JY, Liljegren SJ, et al (2005) Chlorophyll breakdown in senescent Arabidopsis leaves: characterization of chlorophyll catabolites and of chlorophyll catabolic enzymes involved in the degreening reaction. Plant Physiol **139:** 52–63

Roca M, James C, Pružinská A, Hörtensteiner S, Thomas H, Ougham H (2004) Analysis of the chlorophyll catabolism pathway in leaves of an introgression senescence mutant of *Lolium temulentum*. Phytochemistry **65:** 1231–1238

Smart CM (1994) Gene-expression during leaf senescence. New Phytol **126:** 419–448

Smith P, Krohn R, Hermanson G, Mallia A, Gartner F, Provenzano M, Fujimoto E, Goeke N, Olson B, Klenk D (1985) Measurement of protein using bicinchoninic acid. Anal Biochem **150:** 76–85

Tanaka A, Tanaka R (2006) Chlorophyll metabolism. Curr Opin Plant Biol **9:** 248–255

Thomas H (1987) *Sid*: a Mendelian locus controlling thylakoid membrane disassembly in senescing leaves of *Festuca pratensis*. Theor Appl Genet **73:** 551–555

Thomas H, Howarth CJ (2000) Five ways to stay green. J Exp Bot **51:** 329–337

Thomas H, Morgan WG, Thomas AM, Ougham HJ (1999) Expression of the stay-green character introgressed into *Lolium temulentum* ceres from a senescence mutant of *Festuca pratensis*. Theor Appl Genet **99:** 92–99

Thomas H, Stoddart L (1975) Separation of chlorophyll degradation from other senescence processes in leaves of a mutant genotype of medow fescue (*Festuca pratensis* L.). Plant Physiol **56:** 438–441

Todorov DT, Karanov EN, Smith AR, Hall MA (2003) Chlorophyllase activity and chlorophyll content in wild type and *eti 5* mutant of *Arabidopsis thaliana* subjected to low and high temperatures. Biol Plant **46:** 633–636

Tsuchiya T, Ohta H, Okawa K, Iwamatsu A, Shimada H, Masuda T, Takamiya K (1999) Cloning of chlorophyllase, the key enzyme in chlorophyll degradation: finding of a lipase motif and the induction by methyl jasmonate. Proc Natl Acad Sci USA **96:** 15362–15367

Vicentini F, Hörtensteiner S, Schellenberg M, Thomas H, Matile P (1995) Chlorophyll breakdown in senescent leaves—identification of the biochemical lesion in a *stay-green* genotype of *Festuca-pratensis* Huds. New Phytol **129:** 247–252

Wüthrich KL, Bovet L, Hunziker PE, Donnison IS, Hörtensteiner S (2000) Molecular cloning, functional expression and characterisation of RCC reductase involved in chlorophyll catabolism. Plant J **21:** 189–198